Electronic Supplementary Information

Characterization of $La_{1-x}Sr_xMnO_3$ perovskite catalysts for hydrogen peroxide reduction

C. Yunphuttha,[a] S. Porntheeraphat[b], A. Wongchaisuwat[c], S. Tangbunsuk[c], D. W. M. Marr[d] and P. Viravathana[c, e,*]

[a.] Department of Materials Science, Kasetsart University, Bangkok, 10900 Thailand

[b.] Photonics Technology Laboratory, National Electronics and Computer technology Center, Patumthani, 12120 Thailand

[c.] Department of Chemistry, Kasetsart University, Bangkok, 10900 Thailand

[d.] Chemical and Biological Engineering Department, Colorado School of Mines, Golden, Colorado, 80401 USA

[e.] Center of Advanced Studies in Tropical Natural Resources, National Research University, Kasetsart University, Bangkok, 10900 Thailand

* Email: fscipdv@ku.ac.th

Experimental Details

Catalyst preparation

$La(NO_3)_3 \cdot 6H_2O$ (>99.9%, Fisher Scientific), $Mn(NO_3)_2 \cdot 6H_2O$ (>99.9%, Panreac Quimica S.A.), $Sr(NO_3)_2$ (99.9%, Ajax Fine Chemicals), citric acid (>99.0%, Ajax Fine Chemicals), and ethylene glycol (>95.0%, Fisher Scientific) were used as-received. Deionized water was used for preparation and dilution of all the solutions. According to the studies of Rabelo *et al.*[1], the manganese citrate solution was prepared from $Mn(NO_3)_2 \cdot 4H_2O$ and citric acid, with citric acid/manganese molar ratio of 3:1, under stirring at 70°C for 2 h. $La(NO_3)_3 \cdot 6H_2O$ and $Sr(NO_3)_2$ were later added per stoichiometry. The resulting solution was subjected to mechanical stirring and heating at 90 °C for 1 h, after which ethylene glycol was added at a 3:2 citric acid/ethylene glycol mass ratio. This solution was subsequently kept under mechanical agitation and heating at 95 °C for 2 h to form polymeric resin which was then heat treated at 300 °C for 2 h.

Subsequently, the precal-LSM_x powders were calcined at 700 °C for 6 h at a heating rate of 2 °C/min in air atmosphere. Final calcined $La_{1-x}Sr_xMnO_3$ (cal-LSM_x) catalysts included $LaMnO_3$ (cal-$LSM_{0.0}$), $La_{0.8}Sr_{0.2}MnO_3$ (cal-$LSM_{0.2}$), $La_{0.6}Sr_{0.4}MnO_3$ (cal-$LSM_{0.4}$), $La_{0.4}Sr_{0.6}MnO_3$ (cal-$LSM_{0.6}$), $La_{0.2}Sr_{0.8}MnO_3$ (cal-$LSM_{0.8}$), and $SrMnO_3$ (cal-$LSM_{1.0}$).

Characterization

Phases of cal-LSM_x catalysts were investigated by XRD (D8 Advance using Cu K_α X-ray tube (λ= 1.54 Å), Bruker). All XRD spectra were recorded step scans from 2θ = 10 to 70˚ in 2θ angle and phases identified using the JCPDS (Joint Committee on Powder Diffraction Standard). To study the oxidation state and phase using XAS, XANES was carried out at the *K*-edge of manganese (Mn) and the results were compared with those of Mn reference compounds, including Mn foil (Mn^0), $Mn(NO_3)_2$ (Mn^{2+}), MnO (Mn^{2+}), Mn_2O_3 (Mn^{3+}), MnO_2 (Mn^{4+}), std-$LaMnO_3$ and std-$SrMnO_3$. For further studies of cal-LSM_x catalysts, the La- and Sr-XANES were carried out at the L_3-edge of La and Sr, and results compared to La reference compounds of $La(NO_3)_3$ (La^{3+}), La_2O_3 (La^{3+}) and std-$LaMnO_3$, and Sr reference compounds of $Sr(NO_3)_2$ (Sr^{2+}). Manganese foil was used to calibrate the *K*-edge absorption peak at 6539 eV, vanadium foil was used to calibrate the L_3-edge absorption peak at 5465 eV, and $Sr(NO_3)_2$ was used to calibrate the L_3-edge absorption peak at 1940 eV. X-rays

were monochromatized with a channel-cut Ge (220) crystal monochromator and all XANES spectra recorded in transmission mode using a two-chamber ionization detector.

The oxidation ability of $LSM_{0.0}$ and $LSM_{0.4}$ catalysts was investigated during heating from ambient to 550 ˚C by TR-XANES with precal-$LSM_{0.0}$ and precal-$LSM_{0.4}$ used as starting materials. Experiments were performed with synchrotron radiation at the TR-XAS station, Beam line 2.2 at SLRI. To observe changes in Mn species during oxidation, the Mn *K*-edge XANES spectra was recorded in transmission mode and a Si(111) bent crystal monochromator used to provide the energy dispersive XAS to disperse and focus a range of energies. Transmitted X-rays were simultaneously detected with a linear image N-type metal-oxide-semiconductor (NMOS) sensor as 1000 ms. The Mn foil was used to calibrate the *K*-edge absorption peak at 6539 eV. TR-XANES of precal-$LSM_{0.0}$ and precal-$LSM_{0.4}$ were carried out at the Mn *K*-edge and compared to the same Mn reference compounds as on. Catalysts were oxidized by heating from ambient to 550 °C at a heating rate of 2°C/min at 1 bar with a N_2:O_2 mixture flow (70:30 ml/min). After reaching 550 °C, samples were held at 550 °C for 120 min before cooling to room temperature.

Oxidation during calcination of precal-$LSM_{0.0}$ and precal-$LSM_{0.4}$ was investigated via TPO by heating from ambient temperature to 750 ˚C at a heating rate of 5 ˚C/min and then held for 120 min under an O_2 atmosphere of 5.27% in helium at a flow rate of 20 ml/min.

Nitrogen sorption isotherms were performed at -196 °C with an ASAP 2020 sorption analyzer. Prior to the measurements, the samples were degassed at 150 °C overnight. The specific surface areas of samples were calculated using the Brunauer-Emmett-Teller (BET) method at the relative pressure of 0.30. The pore size (D_p) distribution was obtained using the Barrett-Joyner-Halenda (BJH) method on the desorption branches of the isotherms. The total pore volume (V_p) was calculated at a relative pressure of 0.996. The specific surface area from BET (S_{BET}), D_p and V_p were presented in Table S3.

Electrochemical measurement

A LSM_x electrode was prepared by directly spraying the catalyst ink onto the nickel-coated printed circuit board as a substrate, with the active area dimensions of 1x1 cm^2. In this preparation, the total dried mass of 0.3 g of catalyst ink was

composed with 80 %wt cal-LSM_x catalyst, 10 %wt conductive carbon black (N236 Carbon black, Thai Carbon Black Public Co., Ltd.), and 10 %wt Nafion resin (5 %wt, in lower aliphatic alcohols and 15-20 %wt water, Sigma-Aldrich). It was then dissolved in 3.4 ml of ethanol and sonicated for 30 min. After baking at 120 ˚C for 2 h, the catalyst ink was loaded, having about 2-3 mg/cm^2, for each electrode.

Electrochemical measurements were performed using a three-electrode system with an Ag/AgCl reference electrode using saturated KCl as internal electrolyte and a platinum rod counter electrode. Open circuited potential (OCP) and cyclic voltammetry (CV) were obtained using a potentiostat/galvanostat (Autolab PGSTAT 302N, Metrohm Autolab B.V.). The CV of each LSM_x electrode was measured between -1.0 V and 0.0 V using a N_2-bubbled 0.5 M KOH electrolyte and between -0.85 V and -0.2 V using a N_2-bubbled 0.5 M KOH electrolyte containing 0.1 M H_2O_2, at the scan rate of 50 mV/s. Before recording the final voltammogram, the LSM_x electrode was polarized for five runs between -1.0 V and 0.0 V at a scan rate of 50 mV/s in a N_2-bubbled 0.5 M KOH electrolyte. OCP determination was recorded for 20 min. Ultra-pure water (18.3 MΩ/cm-resistivity, Millipore) was employed for preparing electrolytes: the N_2-bubbled 0.5 M KOH with and without 0.1 M H_2O_2.

- Determination of polarization resistance and exchange current density

The conductivity of an electrode is inversely related to the polarization resistance (R_p) which is defined by the following equation:

$$R_p = \left(\frac{\Delta E}{\Delta j} \right)_{\Delta E \to 0}$$

where, ΔE is the applied potential around the corrosion potential or OCP and Δj is the polarization current density. R_p value can be calculated by taking the inverse slope of the polarization current curve at the corrosion potential or OCP. In this experiment, R_p was estimated from cathodic scan of voltammograms of polarized LSM_x recorded in 0.5 M KOH electrolyte (Figure 7(a)), at the applied potential around OCP (-0.020 V). As shown in Figure S3, the slope of the cathodic curve at -0.020 V can be calculated by performing a linear regression on current density from -0.030 V to – 0.010 V (changed the applied potential by 10 mV from -0.020 V, thus, ΔE = (-0.01) – (-0.03) = 0.02 V). The R_p values were collected in Table S3.

- Determination of roughness factor and specific active surface area

The roughness factor (R_f) of the electrode was determined by voltammetry method [2,3]. In this method, the charging current density of double layer capacitance (j_{dl}) is measured at different scan rate ($\upsilon = dE/dt$), as shown in the inset of Figure S7. A slope of a linear relation between j_{dl} and υ is used to determine the double layer capacitance of the electrode (C_{dl}), as shown in Figure S7, according to the equation, where Q is the charge transferred.

$$C_{dl} = dQ/dE = j_{dl}/(\frac{dE}{dt}) = j_{dl}/\upsilon$$

$$R_f = \frac{|C_{dl}|}{60\,\mu F/cm^2}$$

The R_f value was determined, using 60 $\mu F/cm^2$ as the double layer capacitance for smooth oxide surface[4,5] , and the R_f value per mg of the LSM_x mass are displayed in Table S3.

The specific active surface area of electrode was determined from R_f x geometrical area of electrode (1x1 cm^2, in this case), as collected in Table S3.

- Determination of exchange current density

Catalytic activity of H_2O_2 reduction on LSM_x is directly related to the exchange current density (j_0) which can be determined from the cathodic Tafel plot of LSM_x in 0.5 M KOH electrolyte containing 0.1 M H_2O_2, at scan rate of 50 mV/s, as shown in Figure S8. The cathodic Tafel plot is constructed by the following equation:

$$\log|j| = \log|j_0| \frac{\alpha_c n_\alpha F}{2.3RT} \eta$$

where j is current density (A/cm^2), j_0 is the exchange current density, α_c is the cathodic transfer coefficient, n_α is the total number of electron involved in the rate determining step and all previous step, and η is the overpotential (V). The j_0 value was determined from the intercept of the line between η and log j. To get a better consideration on catalytic activity of H_2O_2 reduction on LSM_x, the j_0 value was divided by roughness factor (R_f) for eliminating geometric and electronic effects, and defining as the true exchange current density (j_{0t}), as shown in Table S3.

Sample	Pre-edge energy (eV)	E^0 (eV)	Sample	Pre-edge energy (eV)	E^0 (eV)	Sample	Pre-edge energy (eV)	E^0 (eV)
std-Mn foil	-	6539.0	precal-$LSM_{0.0}$	6541.0	6552.2	cal-$LSM_{0.0}$	6541.9	6553.5
std-$Mn(NO_3)_2$	6540.4	6547.2	precal-$LSM_{0.2}$	N/A	N/A	cal-$LSM_{0.2}$	6542.2	6553.5
std-MnO	6540.4	6550.2	precal-$LSM_{0.4}$	6540.9	6551.9	cal-$LSM_{0.4}$	6542.3	6553.8
std-Mn_2O_3	6540.9	6551.6	precal-$LSM_{0.6}$	6540.9	6551.8	cal-$LSM_{0.6}$	6542.7	6554.1
std-MnO_2	6542.8	6554.2	precal-$LSM_{0.8}$	6540.3	6548.1	cal-$LSM_{0.8}$	6542.9	6554.6
std-$LaMnO_3$	6541.5	6553.4	precal-$LSM_{1.0}$	6540.3	6547.8	cal-$LSM_{1.0}$	6540.8, 6543.3	6555.0
std-$SrMnO_3$	6541.0, 6543.3	6555.3						

Table S1 The Mn *K*-edge for Mn reference and LSM_x compounds determined from the pre-edge peak and the absorption edge energy (E^0).

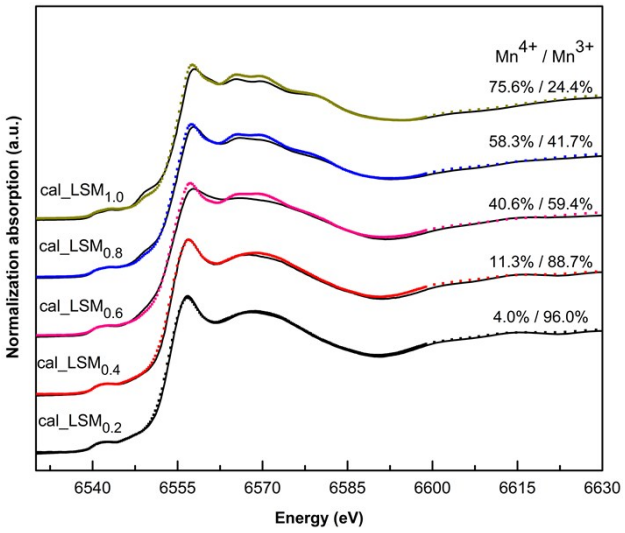

Figure S1 Normalized Mn K-edge XANES spectra of cal-LSM_x and their XANES linear combination fit (LCF) results (fitting range: -20 to100, — experimental data and ···· LCF result).

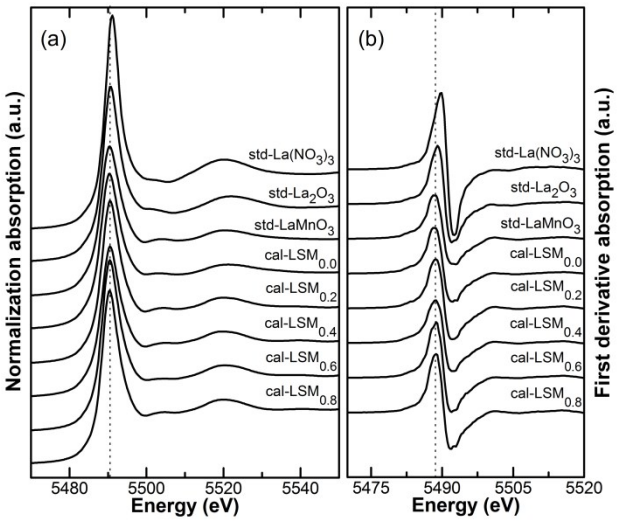

Figure S2 La L_3-edge XANES spectra for cal-LSM_x ($0 \leq x \leq 0.8$) powders, calcined at 700 ˚C for 6 h, and La reference compounds plotted (a) as energy and (b) as first derivative.

The XANES spectra of all cal-LSM_x and La reference compounds, including std-$La(NO_3)_3$, std-La_2O, and std-$LaMnO_3$, are shown in Figure S2(a). From the first derivative plot in Figure S2(b), the E^0 of the La reference standard are 5488.2, 5489.7, and 5489.0 eV for std-$LaMnO_3$, std-$La(NO_3)_3$, and std-La_2O_3, respectively. All spectra exhibited a strong white line La L_3-edge XANES spectra at approximately 5490 eV and were assigned an electronic transition from $2p_{3/2}$ to 5d state.

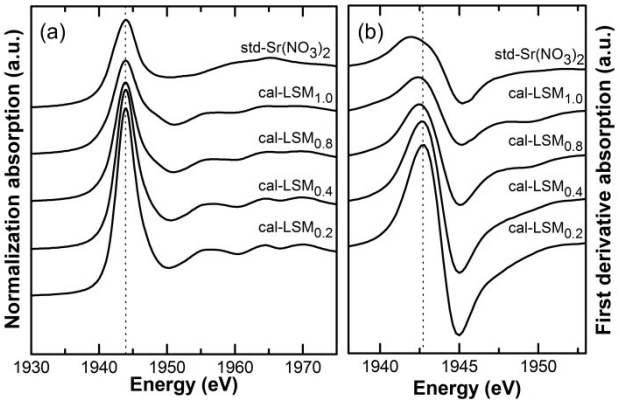

Figure S3 Sr L_3-edge XANES spectra for cal-LSM_x ($0.2 \leq x \leq 1$) powders, calcined at 700 ˚C for 6 h, and La reference compounds plotted (a) as energy and (b) as first derivative.

Normally, XANES spectra as shown in Figure S3(a) are used to identify the average oxidation state of specific elements; however, for the perovskite structure of LSM_x, the oxidation state of Sr is found as Sr^{2+} and no oxidation or reduction reaction can alter this under calcination. From the first derivative plot in Figure S3(b), the E^0 of std-$Sr(NO_3)_2$ is 1941.90 eV and 1942.7, 1942.7, 1942.5, and 1942.4 eV, for cal-$LSM_{0.2}$, cal-$LSM_{0.4}$, cal-$LSM_{0.8}$, and cal-$LSM_{1.0}$, respectively. With increasing Sr doping, the E^0 shift in the Sr-XANES spectra was not observed. Lower white line intensities of the cal-LSM_x catalyst with increasing Sr doping is due to higher Sr concentrations[6].

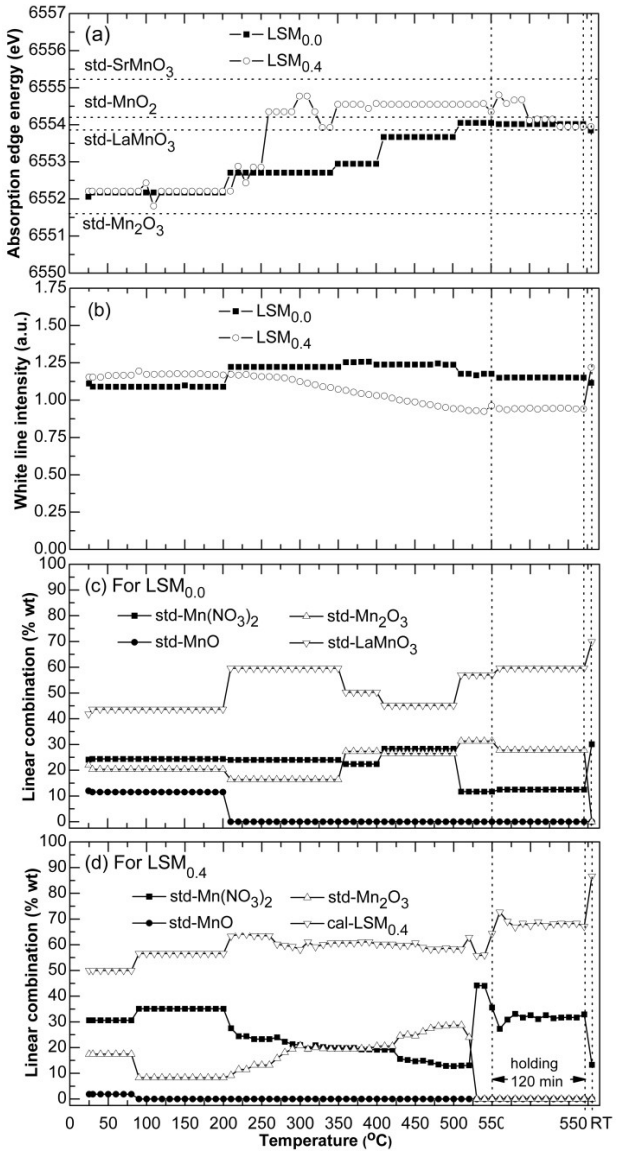

Figure S4 (a) White line intensity and (b) absorption edge energy of Mn and percentage of the Mn references: std-$Mn(NO_3)_2$, std-MnO, std-Mn_2O_3, std-$LaMnO_3$ and cal-$LSM_{0.4}$, as a function of temperature for (c) $LSM_{0.0}$ and (d) $LSM_{0.4}$ catalysts.

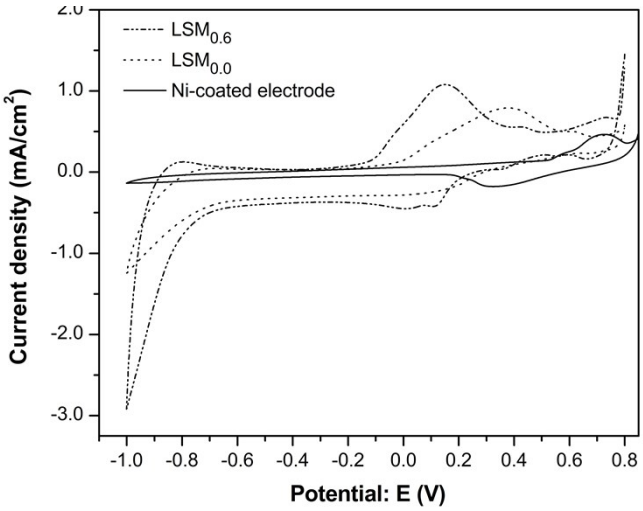

Figure S5 Cyclic voltammogram of $LSM_{0.0}$, $LSM_{0.6}$ and Ni-coated electrodes in the N_2-bubbled 0.5 M KOH electrolyte without 0.1 M H_2O_2 at scan rate of 50 mV/s.

Electrode	OCP Value (mV)			
	N_2-Bubbled 0.5M KOH		N_2-Bubbled 0.5M KOH +0.1 M H_2O_2	
	Fresh electrode	Polarized electrode	Fresh electrode	Polarized electrode
$LSM_{0.0}$	-6.53±0.18	-6.53±0.65	19.31±0.74	27.56±0.20
$LSM_{0.2}$	-11.10±0.27	-3.45±0.42	19.62±0.98	30.36±0.10
$LSM_{0.4}$	-10.10±0.47	-22.21±0.48	22.98±1.30	33.94±0.74
$LSM_{0.6}$	2.92±0.84	-24.45±1.31	29.14±1.46	42.33±0.70
$LSM_{0.8}$	7.83±0.67	-52.83±1.95	23.07±1.43	37.69±0.86
$LSM_{1.0}$	-0.83±0.72	-7.48±1.47	50.75±0.13	53.34±1.05

Table S2 OCP values for LSM_x electrodes in N_2-bubbled 0.5 M KOH electrolyte solution with and without 0.1 M H_2O_2.

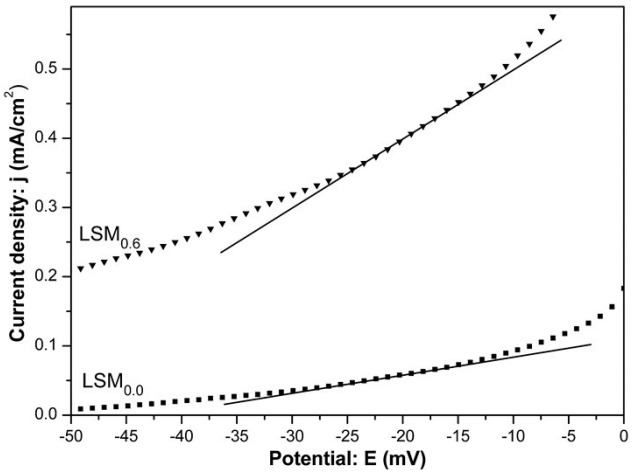

Figure S6 Polarization resistance by plotting cathodic scan of $LSM_{0.0}$ and $LSM_{0.6}$, as representatives of LSM_x in the N_2-bubbled 0.5 M KOH electrolyte, in the potential region of 0 mV to -50 mV at scan rate of 50 mV/s.

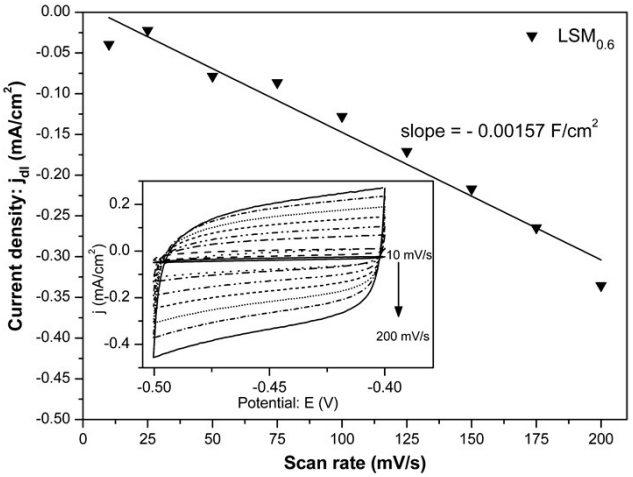

Figure S7 Double layer capacitance of $LSM_{0.6}$ electrode by plotting charging current density at -0.45 V versus scan rate; typical cyclic voltammograms of $LSM_{0.6}$ electrode (geometrical area = 1.0 cm^2) in the potential region, -0.4 V to -0.5 V in 0.5 M KOH and at varying scan rate (10 – 200 mV/s), as shown in inset.

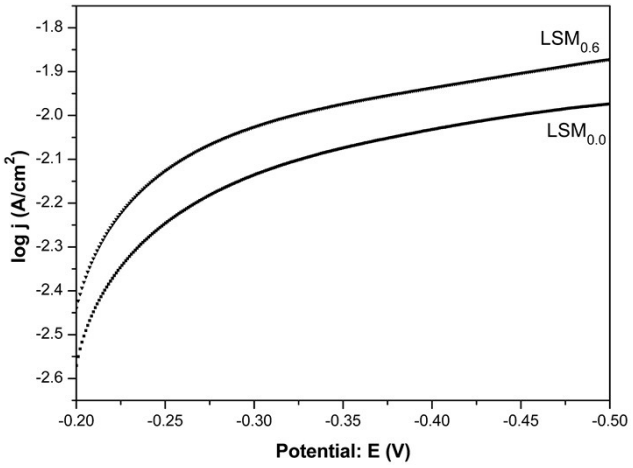

Figure S8 Typical cathodic Tafel plot of $LSM_{0.0}$ and $LSM_{0.6}$ electrode, as representatives of LSM_x, in the potential region, -0.2 V to -0.5 V in N_2-bubbled 0.5 M KOH electrolyte containing 0.1 M H_2O_2.

Electrode	Polarization resistance: R_p ($\Omega \cdot cm^2$)	Roughness factor: R_f (mg^{-1})	Specific active surface area (m^2/g)	Exchange current density (mA/cm^2)		Nitrogen sorption analysis		
				j_0	$j_{0t} = j_0/R_f$	S_{BET} (m^2/g)	D_p (nm)	Vp (cm^3/g)
$LSM_{0.0}$	371.61	49.8	4.98	4.74	0.095	17.76	30.87	0.137
$LSM_{0.2}$	174.37	43.3	4.33	5.24	0.121	n/a	n/a	n/a
$LSM_{0.4}$	153.03	38.8	3.88	5.61	0.145	15.43	39.49	0.152
$LSM_{0.6}$	121.35	37.4	3.74	6.52	0.175	20.81	32.96	0.172
$LSM_{0.8}$	123.06	36.4	3.64	2.41	0.066	n/a	n/a	n/a
$LSM_{1.0}$	156.83	26.5	2.65	2.71	0.103	n/a	n/a	n/a

Table S3 Kinetic parameters for H_2O_2 reduction on LSM_x electrodes in N_2-bubbled 0.5 M KOH electrolyte.

References

1 A. A. Rabelo, M. C. De Macedo, D. M. D. A. Melo, C. A. Paskocimas, A. E. Martinelli and R. M. Do Nascimento, *Mater. Res.*, 2011, **14**, 91–96.

2 R. N. Singh, T. Sharma, A. Singh, Anindita, D. Mishra and S. K. Tiwari, *Electrochim. Acta*, 2008, **53**, 2322–2330.

3 S. J. Amirfakhri, D. Binny, J. L. Meunier and D. Berk, *J. Power Sources*, 2014, **257**, 356–363.

4 J. O. Bockris, *J. Electrochem. Soc.*, 1984, **131**, 290.

5 S. K. Tiwari, P. Chartier and R. N. Singh, *J. Electrochem. Soc.*, 1995, **142**, 148–153.

6 K.-C. Chang, B. Yildiz, D. Myers, J. D. Carter and H. You, *ECS Trans.*, 2009, **16**, 23–31.